Geological Society of America
Special Paper 356
2002

Cretaceous-Tertiary boundary sequence in the Cacarajicara Formation, western Cuba: An impact-related, high-energy, gravity-flow deposit

Shoichi Kiyokawa
Department of Geology, National Science Museum of Tokyo, 3-23-1, Hyakunin-cho, Shinjuku-ku, Tokyo 169-0073, Japan
Ryuji Tada
Department of Earth and Planetary Science, Graduate School of Science, University of Tokyo, 7-3-1 Hongo, Tokyo 113-0033, Japan
Manuel Iturralde-Vinent
Museo Nacional de Historia Natural, Obispo No. 61, Plaza de Armas, La Habana Vieja 10100, Cuba
Takafumi Matsui
Eiichi Tajika, Shinji Yamamoto, Tetsuo Oji,
Youichiro Nakano, Kazuhisa Goto, and Hideo Takayama
Department of Earth and Planetary Science, Graduate School of Science, University of Tokyo, 7-3-1 Hongo, Tokyo 113-0033, Japan
Dora Garcia Delgado
Consuelo Diaz Otero
Instituto de Geologia y Paleontologia Via Blanca y Linea del Ferrocarril San Miguel del Padron, La Habana 11 000, Cuba
Reinaldo Rojas Consuegra
Museo Nacional de Historia Natural, Obispo No. 61, Plaza de Armas, La Habana 10100, Cuba

ABSTRACT

The Cacarajicara Formation of western Cuba is a more than 700 m thick calcareous clastic sequence that contains shocked quartz throughout, and spherules. Three members are recognized. The lower member consists of limestone and chert boulders, and disconformably overlies Cretaceous deep-water turbidite. It is characterized by: (1) a grain-supported fabric with only a small amount of matrix, (2) 5–15 cm, well-sorted clasts and occasional boulders, (3) reversely graded, discoidal or rectangular boulders showing a preferred orientation, (4) abundant shallow- and deep-water carbonate clasts in a well-mixed fabric, (5) direct contact between adjacent clasts, and (6) hydrostatic deformation within a black clay matrix. This evidence suggests that the lower member was deposited under conditions of high-density and high-speed laminar flow. The middle member consists of upward graded, massive to well-bedded, homogeneous calcarenite. Unusual fluid-escape structures in the thick calcarenite suggest that this member formed by high-density turbidity suspension. The upper member consists of fine calcarenite mudstone; there is no evidence of bioturbation. We infer that it was deposited from a dilute, low-density suspension.

Kiyokawa, S., Tada, R., Iturralde-Vinent, M., Masui, T., Tajika, E., Gracia Delgado, D., Oji, T., Nakano, Y., Goto, H., Takayama, H., and Rojas-Consuegra, R., 2002, More than 700-m-thick Cretaceous-Tertiary boundary sequence of the Cacarajicara Formation, western Cuba; Ejecta induced high-energy flow deposit, *in* Koeberl, C., and MacLeod, K.G., eds., Catastrophic Events and Mass Extinctions: Impacts and Beyond: Boulder, Colorado, Geological Society of America Special Paper 356, p. 125–144.

On the basis of these criteria, the Cacarajicara Formation is interpreted to be a single hyperconcentrated flow that was formed by high-energy and high-speed concentrated flow. The south-southeast paleocurrent direction suggests that this high-energy flow originated on the Yucatan platform and was triggered by the Chicxulub impact. We propose that a gigantic flow deposit was induced by earthquake-generated collapse of the Yucatan platform margin owing to ballistic flow from the Chicxulub impact.

INTRODUCTION

Impact-related sedimentary deposits have been described at Cretaceous-Tertiary (K-T) boundary sites in the Yucatan Peninsula region (e.g., Pope et al., 1999). In addition, coarse clastic sequences of impact origin have been reported from marginal areas of the adjoining Gulf of Mexico (e.g., Smit, 1999), and are inferred tsunami or gravity flow deposits (Bourgeois et al., 1988; Bohor, 1996; Smit et al., 1996). In the central Gulf of Mexico and Caribbean Sea, debris-flow deposits at some Ocean Drilling Program sites have been interpreted as originating from a collapsed platform margin (Alvarez et al., 1992; Bralower et al., 1998). Proximal deposits of impact origin have also been discovered east and south of the Yucatan Peninsula. The nearest such outcrop is on Albion Island, Belize, ~350 km south of the Chicxulub crater (Ocampo et al., 1996; Pope et al., 1999). The East Yucatán oil field, which is located 350–600 km from the crater, contains a thick layer of impact ejecta and clasts (Grajales-Nishimura et al., 2000). Deep core data from the crater have revealed detailed characteristics (Hildebrand et al., 1991; Sharpton et al., 1996). However, the record from the continental shelf to the oceanic basin on the east and south side of the Yucatan Peninsula is still poorly known.

Western Cuba consists of a Paleogene orogenic belt formed by interaction between the North American and Caribbean plates (Pindell and Barrett, 1990; Ross and Scotese, 1988; Gordon et al., 1997). The orogenic belt in western Cuba contains Late Cretaceous to early Tertiary sequences that include a thick, well-preserved late Maastrichtian section consisting of the Cacarajicara and Peñalver Formations (Pszczolkowski, 1986; Bohor and Seitz, 1990; Piotrowska, 1993; Iturralde-Vinent, 1992, 1994a, 1994b, 1996). The depositional environments and trigger events for these unusually thick formations have been discussed, and several origins have been proposed, including orogenic-volcanic debris deposits, impact-related ejecta, tsunami deposits, and earthquake-related megaturbidites (e.g., Palmer, 1945; Pszczolkowski, 1986; Bohor and Seitz, 1990; Iturralde-Vinent, 1992; Takayama et al., 2000). End-Cretaceous plate reconstructions (Iturralde-Vinent, 1994a) indicate that the study site was situated near the eastern margin of the Yucatan Peninsula, and may preserve proximal evidence related to the K-T impact.

In this chapter we describe the lithologic characteristics of the unusually thick Cacarajicara Formation, focusing especially on the lower member, which contains a thick clastic sequence. We also discuss the possible depositional mechanisms responsible for this thick sequence.

REGIONAL GEOLOGIC SETTING

From Cretaceous to Eocene time, the Cuban island arc moved northeastward along the southeast margin of the Yucatan Peninsula (Fig. 1) (Pindell et al., 1988; Ross and Scotese, 1988). Fragments of the Yucatan block were detached and moved at least 350 km by left-lateral transform motion in the Paleocene to early Eocene and formed the Guaniguanico terrane (Rosencrantz, 1990; Iturralde-Vinent, 1994b). The Cretaceous Cuban island arc finally collided with the North American continent and formed a collisional fold and thrust belt (Iturralde-Vinent, 1994a, 1994b; Gordon et al., 1997). The orogeny in western Cuba was characterized by collision and strike-slip deformation during the Paleocene and early Eocene and resulted in very complex geology (Gordon et al., 1997).

Western Cuba consists of the Pinos and Guaniguanico terranes (Iturralde-Vinent, 1994a; Kerr et al., 1999). The Pinos terrane is a medium pressure–medium temperature metamorphic sialic complex. The Guaniguanico terrane contains ophiolite-bearing thrust-nappe sequences of Paleocene to early Eocene age (e.g., Cajalbana ophiolite: Pszczolkowski, 1994), and was strongly affected by Paleocene–middle Eocene strike-slip deformation during the opening of the Yucatan basin (Rosencrantz, 1990). The Guaniguanico terrane consists of several tectonic belts, one of which is the Rosario belt (Iturralde-Vinent, 1996). The Rosario stratigraphic sections include continental slope and rise hemipelagic deposits of Late Jurassic to Late Cretaceous age, as well as Paleocene and Eocene foreland deposits (Pszczolkowski, 1978, 1994; Iturralde-Vinent, 1994b; Bralower and Iturralde-Vinent, 1997). The Guaniguanico terrane is overlain by ophiolites and volcano-sedimentary rocks of the Bahía Honda–Matanzas allochthon. Well-preserved K-T boundary sequences in western Cuba include the Moncada Formation in the Los Organos belt (Tada et al., this volume), the Cacarajicara Formation in the Rosario belt, and the Peñalver Formation in the Bahía Honda–Matanzas allochthon (Takayama et al., 2000).

The study area is located near Loma Cornelia, along the road from Soroa to Bahía Honda, ~10 km north of the town of Soroa. There are excellent outcrops along an adjacent river,

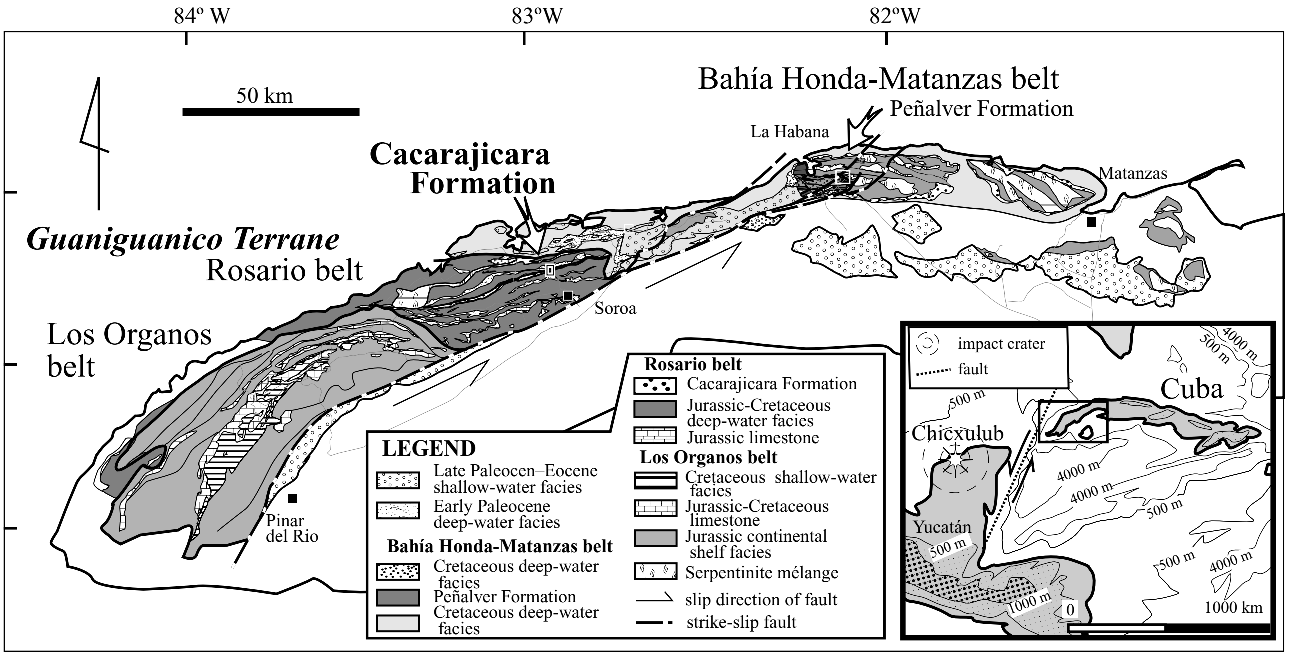

Figure 1. Geologic map of western Cuba, showing Guaniguanico terrane and location of Cacarajicara Formation outcrops (after Pushcharovsky, 1989). Map on right shows location of western Cuba and Yucatan Peninsula, with respect to buried Chicxulub impact crater and topographic centerlines. Dashed circles represent proposed crater diameters: 180 km (Hildebrand et al., 1991) and 300 km (Sharpton et al., 1992, 1996).

where we conducted mapping and sampling (Fig. 2). We sampled along roadcuts and river bluffs continuously every 5 m vertically, collecting the clasts and matrix in the breccia sequences. Thin sections were prepared, and grain separation was accomplished by dissolution in hydrochloric acid and magnetic separation. More than 100 thin sections of rock chips, and 100 acid-dissolution samples were used to determine the grain type and size, and grain-boundary conditions, by using a petrographic microscope, energy-dispersive spectrometer (EDS; JEOL 5400), and electron probe microanalyzer (EPMA; JXA-8800M) (for details see Yokoyama et al., 1993).

CACARAJICARA FORMATION

The Cacarajicara Formation is present only in the Rosario belt as nearly continuous strips 0.5–1.0 km wide and to 100 km long in an east-west direction (Fig. 1). Latest Maastrichtian rudists, foraminifera, and nannofossils occur in the matrix and in fossil-bearing limestone fragments, but no Paleocene fossils have ever been reported (Pszczolkowski, 1986; Iturralde-Vinent, 1992).

CROSS SECTION

The Cacarajicara Formation dips 70°–80° to the north, as indicated by the thin pebbly layer in the calcarenite (Fig. 3); the pressure-solution cleavage preserved in the calcarenite dips 30° to the north. The lower boundary with the Lower Cretaceous Polier Formation is partly disturbed by a reverse fault that dips 60° south and has steeply plunging lineations. This disconformable (erosional) contact is preserved in the hanging wall of the fault. The upper boundary was disturbed by strike-slip and shear deformation and is overlain by the Paleocene Ancon Formation. The Cacarajicara Formation is underlain by the Santonian?-Campanian-Maastrichtian Moreno Formation or older units at some other localities (Pszczolkowski, 1978, 1994).

LITHOSTRATIGRAPHY

The Cacarajicara Formation is an ~700-m-thick, upward-fining, homogeneous, calciclastic sequence. It can be subdivided into the Lower Breccia, Middle Calcarenite, and Upper Lime Mudstone Members (Fig. 4). The boundaries between the members are gradual; there are no sharp lithologic discontinuities except for the contacts with Eocene sediments.

In order to understand the depositional mechanism for the Cacarajicara Formation, we focused our study on the detailed sedimentary structures and lithologic characteristics, including grain composition, size, shape, and boundaries, and matrix components. We used microscopic point counts for the Middle Calcarenite and the Upper Lime Mudstone Members and outcrop point counts for the Lower Breccia Member. Grain-size variations were determined from 200 counts at one locality in each member.

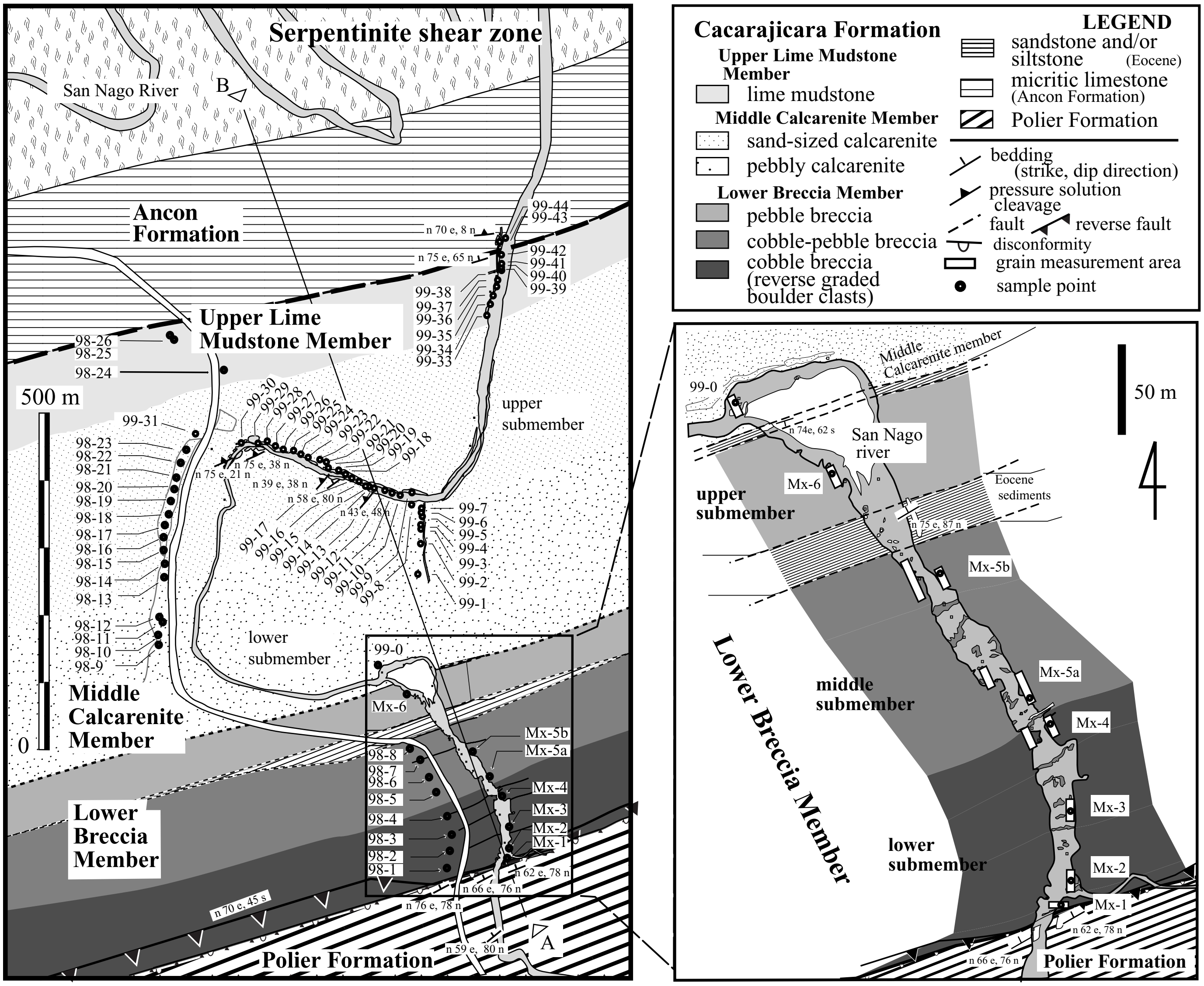

Figure 2. Geologic map of Cacarajicara Formation along San Nago River (left). Geologic map of Lower Breccia Member (right). Black dots and numbers are sampling points and sample number.

Lower Breccia Member

The Lower Breccia Member is more than 250 m thick and is composed of cobble- to pebble-size clasts consisting of shallow- and deep-water limestones, black chert, bedded chert, and greenish shale (Fig. 5, A, B, and C). The breccia is well sorted and grain supported, with only a small amount of matrix. Discoidal or rectangular boulders floating among the cobble-pebble clasts are conspicuous (Fig. 5, B and C).

The Lower Breccia Member is subdivided into the lower, middle, and upper submembers (Fig. 6). The lower submember contains the cobble- to boulder-size breccia and larger boulder clasts (Fig. 5B). The black clay matrix contains some shocked quartz; the matrix in the basal part of this submember contains spherules. The middle submember contains the pebble- to cobble-size breccia; there are no larger boulder clasts (Fig. 5C). The upper submember contains pebble-size breccia; black chert pebbles are more homogeneous in size than in the middle and lower submembers.

Grain composition. More than 50% of the clasts in the Lower Breccia Member are calcareous angular or rounded limestone. The angular limestone is composed of rudist limestone, massive coarse calcarenite, foraminiferal limestone, and micritic limestone with black chert layers. Small amounts of oolitic limestone and calcareous algal mat limestone are also present. The rounded limestone has a more eroded surface than the angular limestone, and is composed of micritic limestone, foraminiferal limestone, and dolostone, 3–10 cm in diameter (Fig. 7).

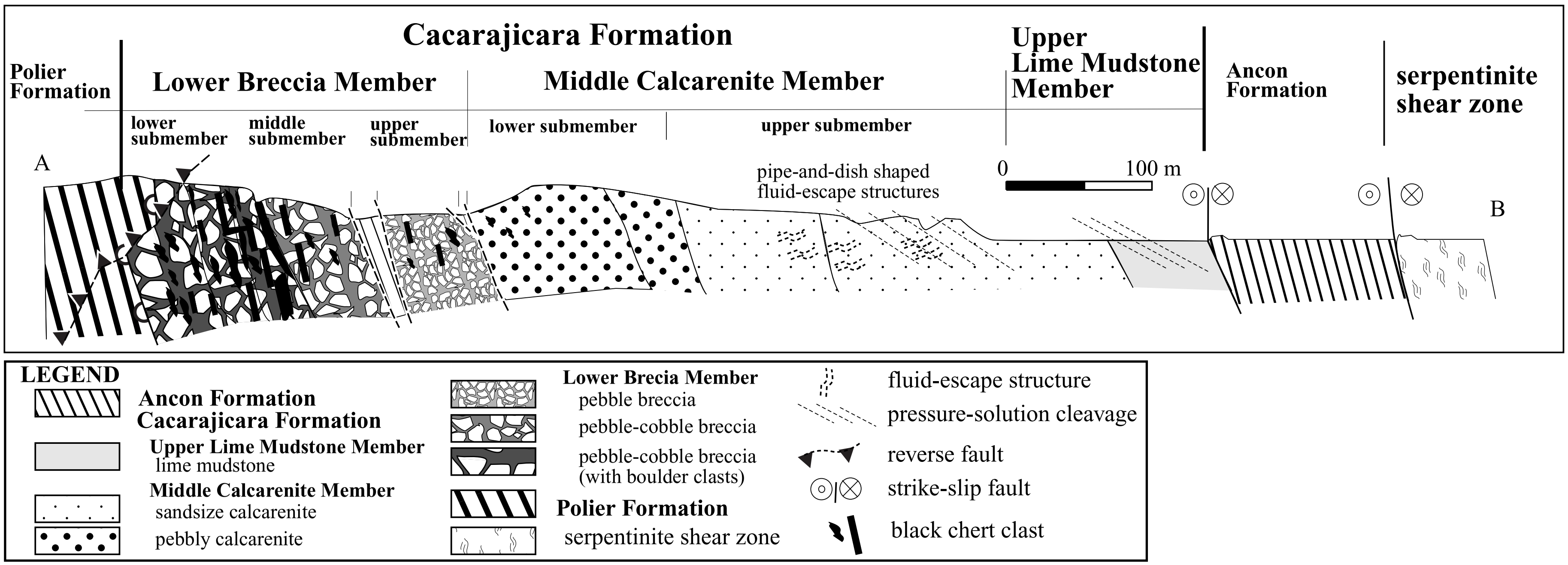

Figure 3. Cross section of Cacarajicara Formation.

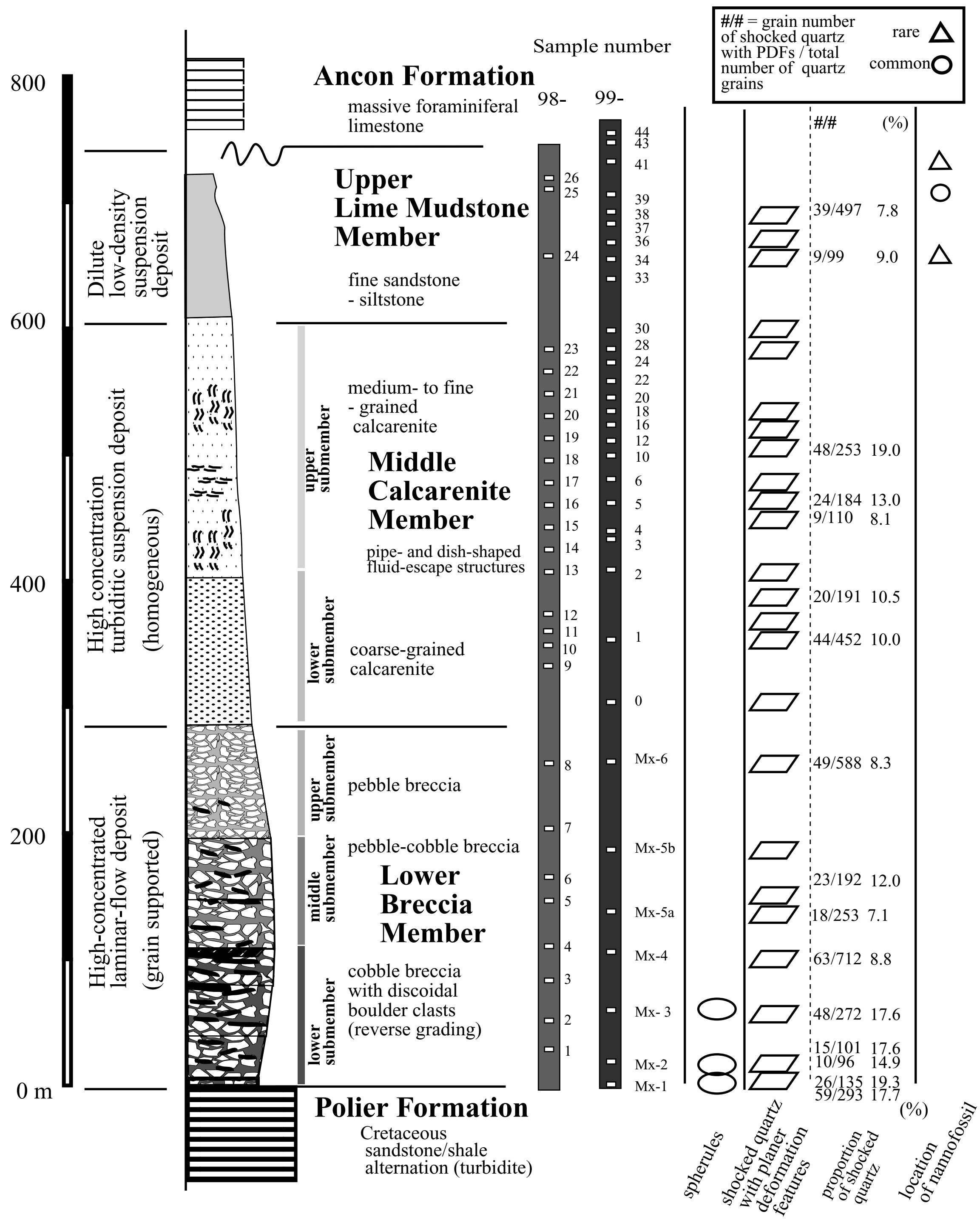

Figure 4. Lithologic column for Cacarajicara Formation. Squares and line of sample numbers indicate points in thin sections where proportion of shocked versus unshocked quartz was counted. Occurrences of spherules, shocked quartz, and nannofossils are shown in right columns. PDF is planar deformation feature.

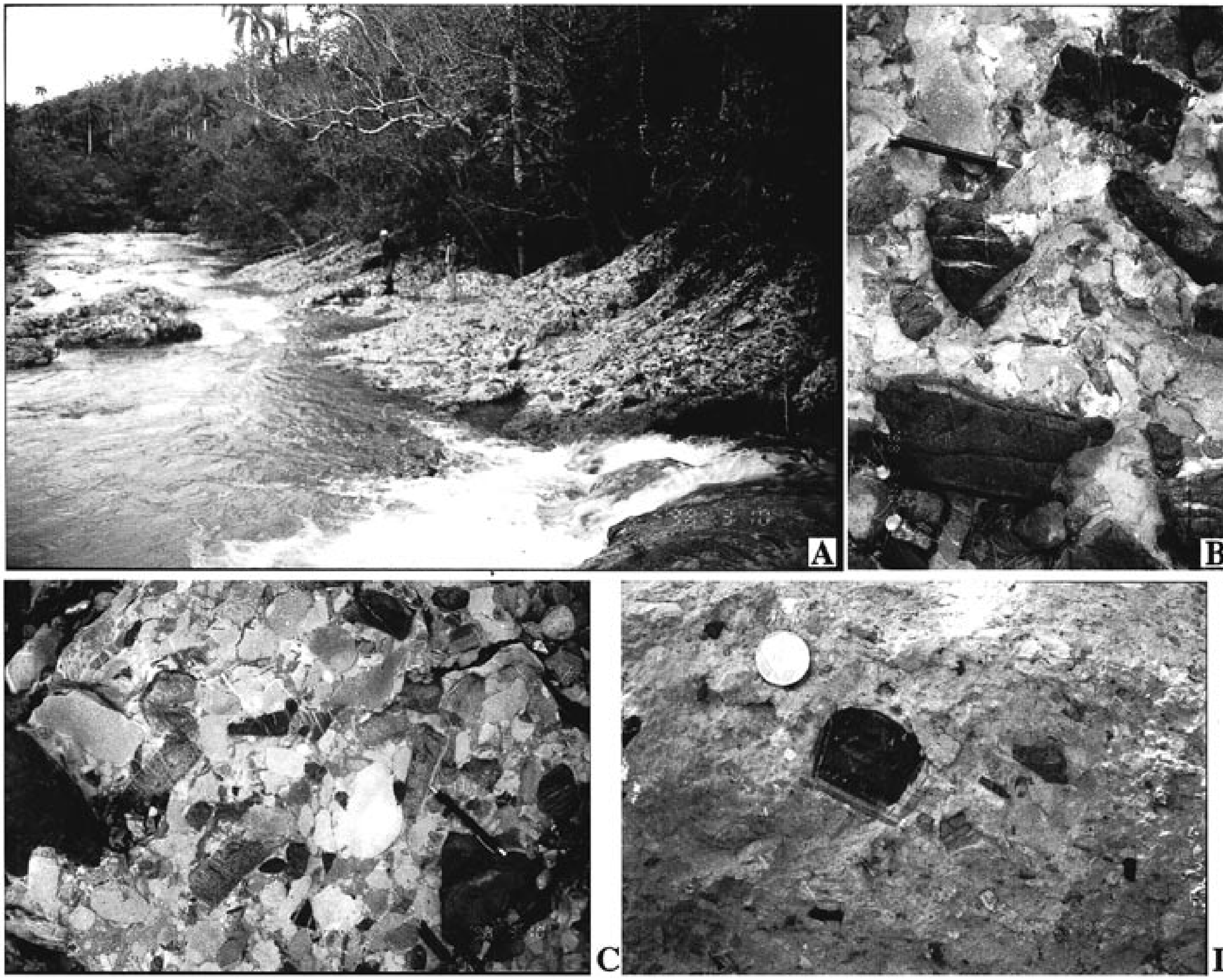

Figure 5. A: Overview of Lower Breccia Member. Continuous outcrop is preserved along Nago River. B: Basal part of Lower Breccia Member. Breccia contains discoidal and/or rectangular clasts of black chert, greenish shale, and gray limestone. Pebble size fraction mainly contains rounded limestone clasts. Matrix in these clasts is very poorly preserved. C: Lower submember of Lower Breccia Member. Note black chert and greenish shale particles preserved in pebbly limestone clast. D: Pebbly calcarenite of lower Middle Calcarenite Member. White margin of black chert clast is replaced by carbonate. E: Elongated fluid-escape pipe structures in homogeneous calcarenite in upper Middle Calcarenite Member. Weak subhorizontal foliation is pressure-solution cleavage. F: Fluid-escape vein structures in homogeneous calcarenite of upper Middle Calcarenite Member. Diffuse webby laminations (slanting to right) of fluid-escape structures are well preserved in this sequence, and resemble structures seen in Peñalver Formation. Lens cap, 55 cm for scale. G: Rectangular bedded red chert clast in uppermost lower submember of Lower Breccia Member. Hammer, 35 cm for scale. H: Black chert clast in upper part of lower submember of Lower Breccia Member. Scale is film cap in center. I: Black siliceous sandstone clast in upper part of lower submember of Lower Breccia Member. Sandstone is 1 m thick and more than 10 m long. Note that there is no fault in this calcarenite.

Chert represents 40% of the pebble- to cobble-size clasts, which consist mainly of black chert (Fig. 5, B, C, and H), black chert associated with foraminiferal limestone, and red radiolarian chert (Fig. 5G). The black chert clasts are similar in lithology to the black chert in the Cretaceous deep-water Pons Formation of the Guaniguanico terrane.

Minor clast components include green shale (Fig. 5G), green altered volcanic rock, trachytic basalt (Fig. 8A), vesicular basic rocks (Fig. 8B), quartz-rich sandstones (Fig. 5I) and pelitic and psammitic schists. The minor grain compositions imply a variable source area within a volcanic and orogenic region.

Grain size and shape. There are two modes of grain sizes in the lower submember of the Lower Breccia Member (Fig 6). The smaller clasts are ~3–15 cm and no size grading is obvious (Fig. 5C); this range composes 60%–70% of this member by

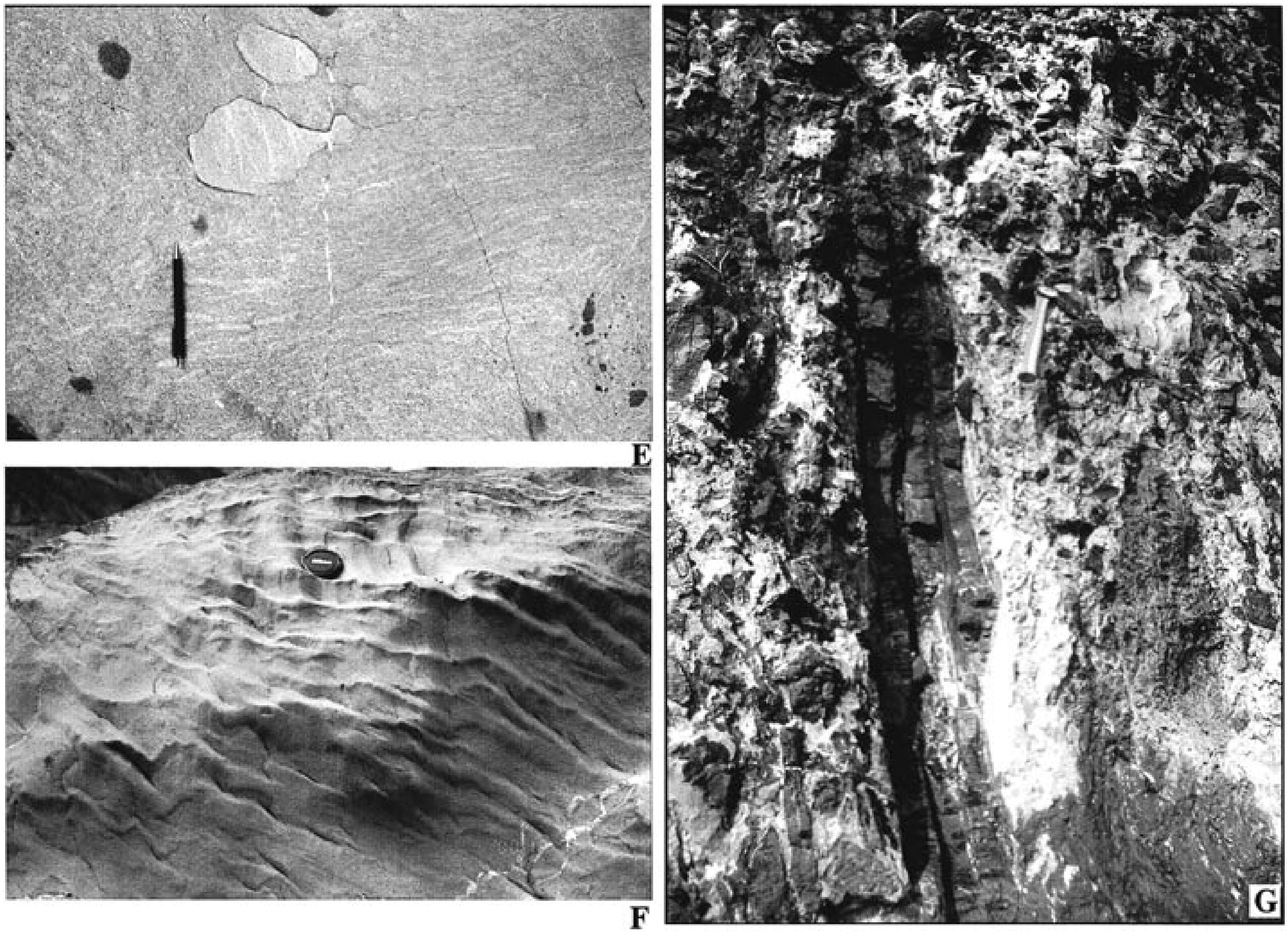

Figure 5. Continued

volume. The larger clasts are 30–300 cm (average long axis 40 cm; Fig. 5G), and compose to 5% by volume; this clast size range exhibits reverse grading (Fig. 6). The uppermost part of the lower submember contains the largest clasts, including some that are >2-m-long, discoidal to rectangular black chert, and others that are >10-m-long, 80-cm-thick, black, less calcareous sandstone blocks (Fig. 5, G, H, and I). The upper and middle submembers lack large boulder clasts in the gradually formed fining-upward sequences.

The largest angular clasts in the Lower Breccia Member were not affected by abrasion. The cobble- to pebble-size carbonate clasts are subrounded and subangular, and have homogeneous compositions. The minor clast components, such as green shale, schist, and volcanic rocks, are mostly <5 cm in diameter and well rounded. They were probably reworked long before deposition in the Cacarajicara Formation.

Grain-boundary condition. The clasts are mostly in direct contact with each other; harder angular grains are partly abraded into softer, rounded limestone clasts (Figs. 5, B and C, and 8D). There are many hydrofractured limestone clasts in the matrix alongside the larger clasts. Cracked chert clasts, matrix clay intrusion structures, and highly brecciated material form a jigsaw puzzle-like mosaic or texture preserved along the limestone clast margins (Figs. 8F and 9, A and B). Some black chert is fractured, and sharp cracks are filled by the general matrix clay (Fig. 8, E and F). Along narrow cracks in the large discoidal boulders, dark brown clay matrix contains brecciated pebbly micritic limestone (Fig. 9A).

Matrix. The matrix composes <1–3 vol% of the Lower Breccia Member, and fills the very narrow spaces between the closely packed clasts. This matrix is composed of dark brown to black clay and some sand-size carbonate fragments. According to EPMA element mapping, there are many dolomite fragments in this clay matrix. The matrix is composed mainly of brown to dark brown clay, and small amounts of sand-size carbonate, siliceous, and opaque grains (Fig. 9C). The basal part

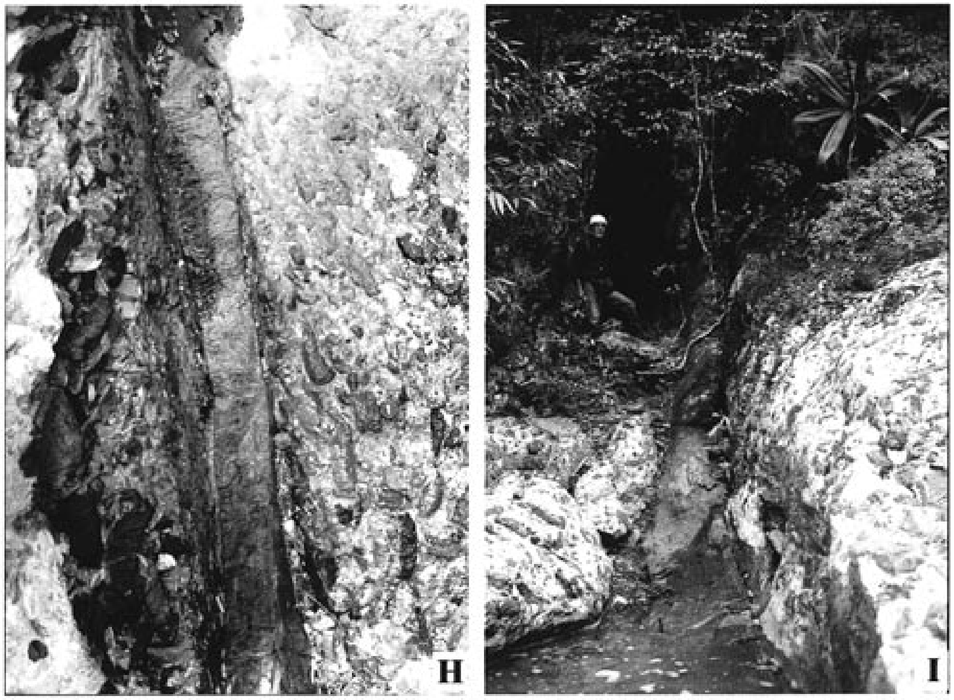

Figure 5. Continued

in this member exhibits an especially low content of limestone grains. Sand-size carbonate grains in the clay matrix increase upsection throughout the Lower Breccia Member.

Middle Calcarenite Member

The ~300-m-thick Middle Calcarenite Member is composed of well-sorted, massive, homogeneous calcarenite, which exhibits upward fining and distribution grading. A partly preserved pebbly bed and parallel laminations are rarely present as bedding in this homogeneous calcarenite. The boundary between the Lower Breccia and the Middle Calcarenite Members is a fault contact within the Eocene turbidite sequence. However, the rock gradually changed to fining upward. Except for the chert grains, the grain composition resembles the upper submember of the Lower Breccia and the lowest Middle Calcarenite Members.

The Middle Calcarenite Member can be subdivided into upper and lower submembers. The lower submember is composed of coarse granular carbonate calcarenite with pebble-size clasts (Fig. 5D). The calcareous sand grains are mainly composed of limestone fragments of rudists, algal mats, and foraminifers. The pebble-size clasts are fragments of black chert, greenish shale, volcanic rocks, and schist. The percentage of pebbly clasts gradually decreases upward.

The upper submember is composed of massive, coarse- to medium-grained, calcareous calcarenite, with a well-sorted and very homogeneous fabric (Fig. 5, E and F). The sand grains are mainly composed of micritic limestone fragments and foraminiferal skeletons, and a smaller amount of larger bioclasts. The massive, coarse calcarenite contains many unusual fluid-escape structures similar to those reported in the Peñalver Formation near Havana (Bronnimann and Rigassi, 1963; Takayama et al., 2000). Fluid-escape structures in this submember are mainly pillar, pipe, and spiral shaped; there are some dish-shaped structures (Fig. 5, E and F).

Grain composition. The calcarenite of the Middle Calcarenite Member consists of more than 85%–90% calcareous grains, including two types of fragments: shallow-water bioclastic limestone, comprising rudists, stromatolites, and oolite, and deep-water fragments of micritic limestone and foraminiferal limestone (Fig. 7). The lower submember mostly contains rudist, bioclastic, and foraminifer limestone fragments, and the upper submember mainly contains foraminiferal grains and micritic limestone (Fig. 7). The remaining 15%–10% of the grains are quartz and feldspar (6%–10%), chlorite-smectite-replaced volcanics or serpentinite (3%–4%), and other minerals (Fig. 7). Single-crystal piemontite, indicative of low- to medium-grade metamorphism, and zircon and chrome spinel are present in the matrix in small amounts.

Calcareous grains compose >80 vol% of both the Cacarajicara and Peñalver Formations, but the relative presence of associate minerals differs significantly. On the basis of the magnetically separated samples from each formation, the Cacara-

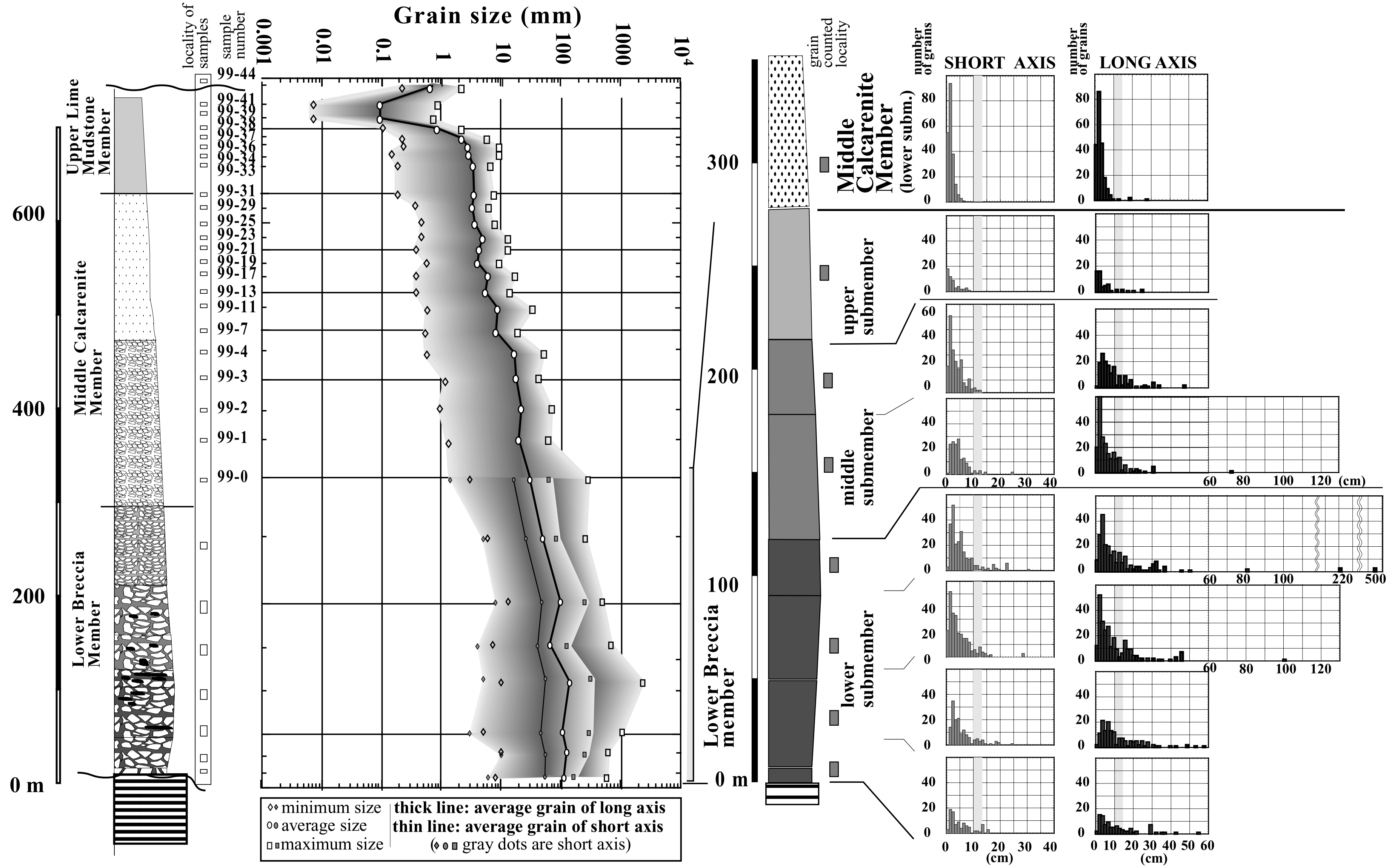

Figure 6. Left: Grain-size distribution of Cacarajicara Formation. There are 33 data points in this sequence. Each data point is based on 200 grains counted to show minimum, average, and maximum size data. Thin-section method used above Middle Calcarenite Member and field-observation method used for Lower Breccia Member. Width of shadow shows grain-size variation. Square and rhombus points show largest and smallest grain sizes, respectively. Darkest part with circle point shows average of grain-size variation. Note that thin and thick lines of Lower Breccia Member show average grain size on short axis and fluctuations on long axis. Right: Detailed grain-size variation diagram of Lower Breccia Member. Note that clasts are of two types: major 3–7 cm size group and minor boulder size group. Sizes of boulder clasts increase from lower to upper in lower submember of Lower Breccia Member.

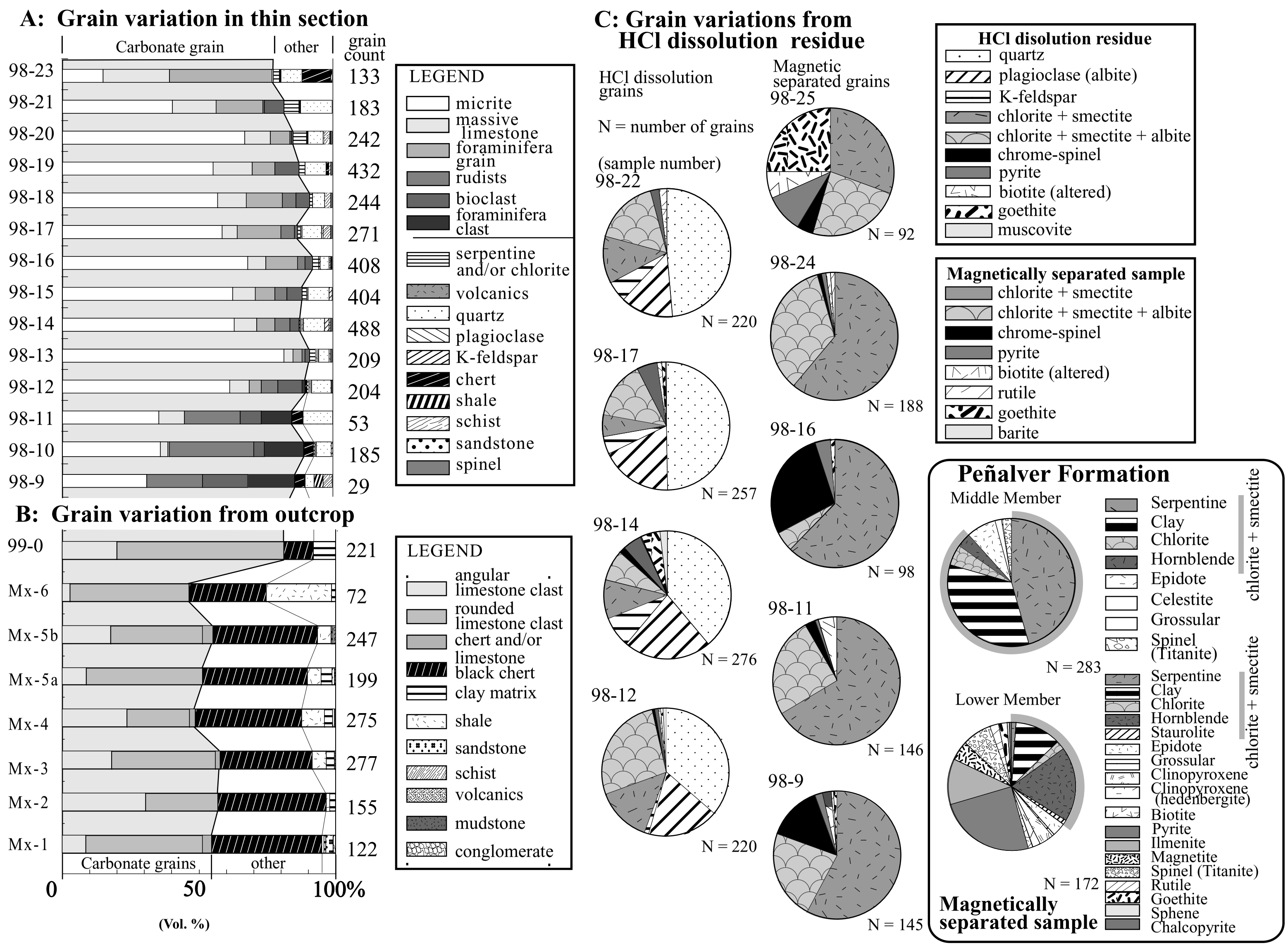

Figure 7. Thin-section and outcrop-scale grain-type variation of nondissolved samples from throughout Cacarajicara Formation (left). Grain composition of HCl dissolution and magnetically separated residue (right). Box on right shows data comparable with Peñalver Formation, which has more variable grains. Considering metamorphic alteration, composition of grains between Cacarajicara and Peñalver Formations is very similar.

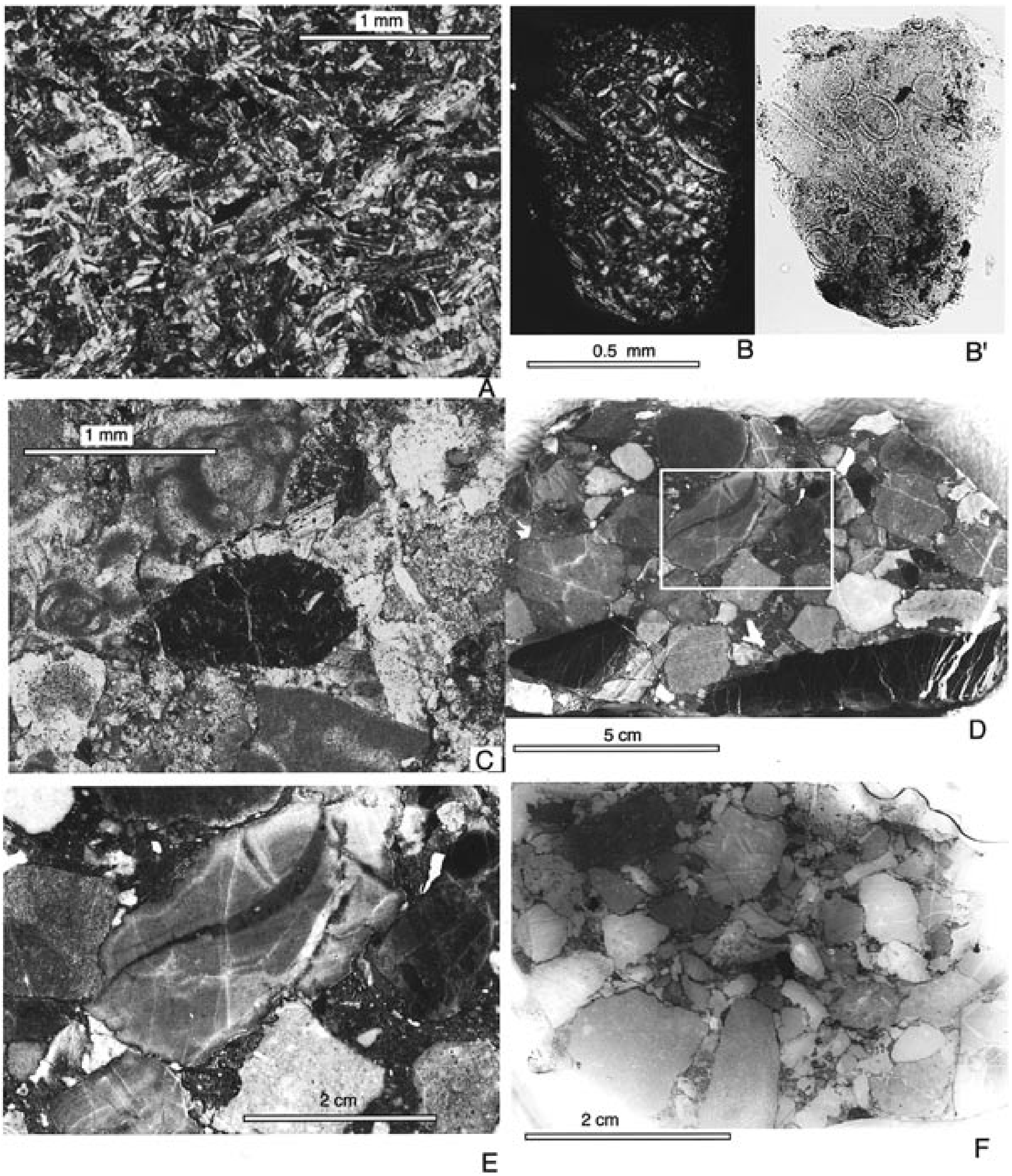

Figure 8. A: Thin-section microphotograph (crossed polarizers) of basaltic clast from lower submember of Lower Breccia Member. B: Thin section of vesicular shard in Middle Calcarenite Member: B, crossed nicols; B', parallel polarizers. Note that grains are filled by chlorite, although some portions of shard are isotropic and may be mostly glass. C: Thin section of well-rounded volcanic grains in coarse calcarenite from Middle Calcarenite Member (plain light). D: Polished section of pebbly clast from Lower Breccia Member. Varied clast types preserved in poor matrix. Rectangle shows E. E: Muddy matrix fills fracture in green chert. F: Polished section of coarse calcarenite of lower Middle Calcarenite Member.

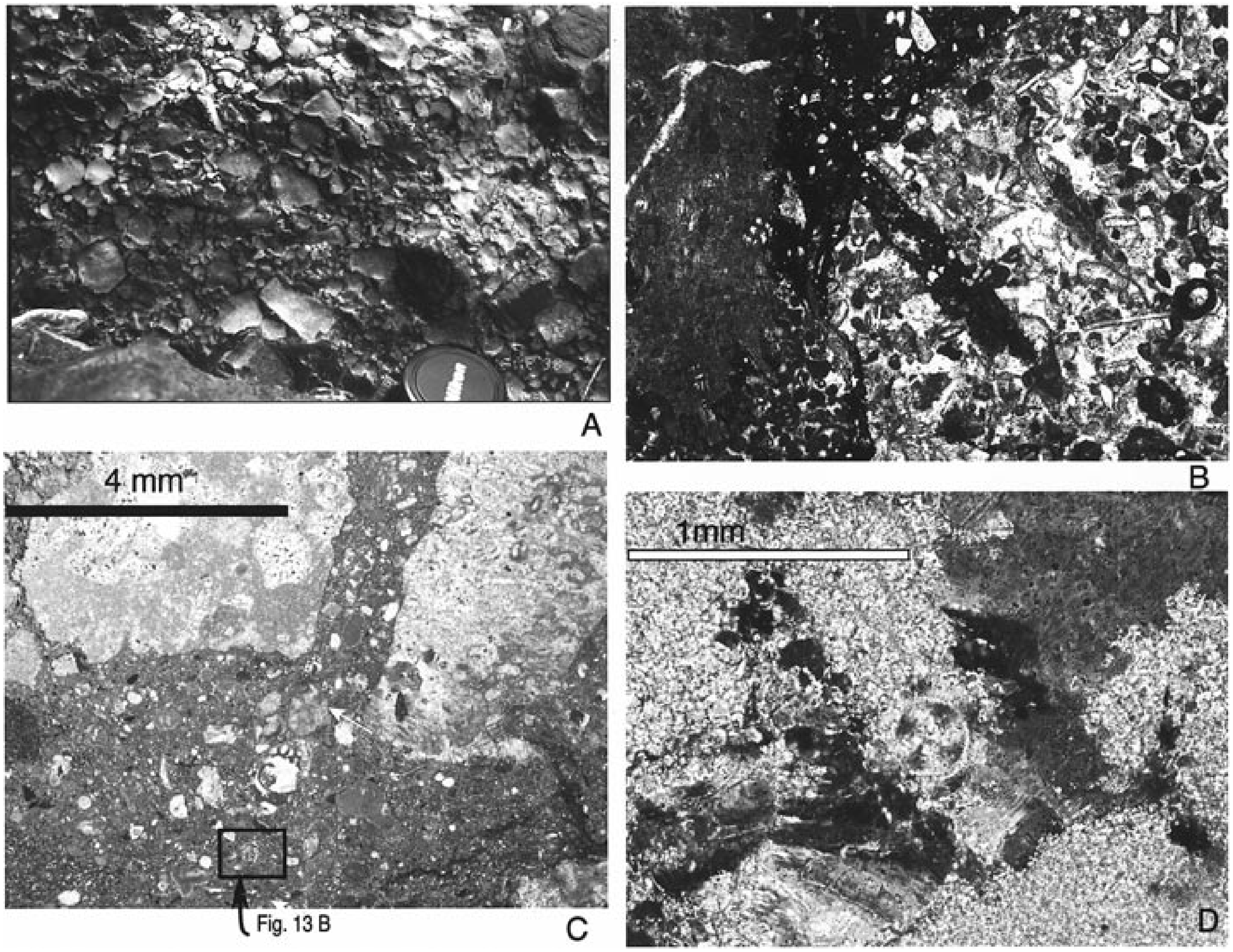

Figure 9. A: Pebbly limestone with black matrix along 3-m-long, disk-shaped clast. Note that limestone float in black matrix has been affected by hydrofracturing. Lens cap, 5.5 cm for scale. B: Thin-section view of margin of limestone grain. Intrusion of matrix preserved in limestone grain in upper submember of Lower Breccia Member (parallel polarizers). C: Thin-section view of matrix from basal part of Lower Breccia Member. Isolated round quartz spherules are preserved. (Square shows more detailed Fig. 13B) E: Microcarbonate pisolith in thin section of medium calcarenite. Pisolith forms radial pattern crystal of carbonate with very thin, spherical shell.

jicara Formation preserved only smectite and chlorite grains, but the Peñalver Formation, especially the middle member, contains serpentine, clay, epidote, chlorite, hornblende, and grossular (Fig. 7). This difference probably reflects the low-grade metamorphism of the Rosario belt. In addition, minerals such as serpentinite, clay, and hornblende may have decomposed or altered to chlorite-smectite minerals (Fig. 7).

Grain size and shape. The calcarenite in this member is well sorted, and the carbonate grains are mainly angular, whereas the volcanic, schist, and shale grains are well rounded. The rounded noncarbonate grains may have a reworked origin. The lower submember contains large fragments of rudist, bioclastic, and foraminiferal limestone. The upper submember contains small grains of foraminifer skeletons and micritic limestone. This size fractionation may have resulted from depositional sorting of the original grains.

Matrix. Matrix is rarely present in the well-sorted calcarenite, and when present it consists of very fine calcareous clay in the narrow spaces between sand-size grains. Calcite pisoliths, 200–300 μm and having very thin skin, are well preserved in the matrix of medium-fine calcarenite. They appears as 10 or more grains seen in 3×4 cm thin sections, and compose $<10\%$ of the matrix.

Upper Lime Mudstone Member

The Upper Lime Mudstone Member is more than 100 m thick, and consists of homogeneous, massive, calcareous, fine

calcarenite and lime mudstone. The lithology gradually changes from that of the underlying Middle Calcarenite Member. The upper boundary with the Paleocene Ancon Formation is a fault contact, and the exact boundary is not observable. This member consists of calcareous, fine calcarenite and lime mudstone with some foraminifer skeletons, shallow-origin bioclasts, and black carbon fragments that might be wood. Foraminifer skeletons are very rare in the uppermost part of this member. Poorly preserved sedimentary structures are present, such as cross-lamination, bioturbation, or fluid-escape structures, in addition to faint parallel bedding. The overlying Ancon Formation contains many foraminifers and exhibits a bioturbation texture.

There are some nannofossils in the limestone (Fig. 4), including *Micula dexussata*, which ranges from Coniacian to Maastrichtian; no Paleocene fossil was found in this member.

PALEOCURRENTS

Imbricated clast structures indicative of paleocurrents are present in the Lower Breccia Member; the discoidal and/or rectangular clasts show flow orientation. We measured the dips and strikes of clasts >40 cm in greatest diameter. The estimated current orientation is corrected for folding; the fold plane dips 80° north with zero plunge of the axis (Fig. 10). The area of Cacarajicara Formation distribution is 100 km long and the lithology is very uniform, and we estimate that the folding plunge in this area is very shallow and not involved in crustal rotation. The disk-shaped clasts preserve imbricated structures, and the paleocurrent evidently flowed from north-northwest to south-southeast in current terms (Fig. 10).

IMPACT EVIDENCE

Shocked quartz and spherules of probable impact origin (e.g., Bohor and Glass, 1995; French, 1998) are present in the Cacarajicara Formation. Carbonate pisoliths are also preserved in the calcarenite, which might be a microcarbonate pisolith (Pope et al., 1999).

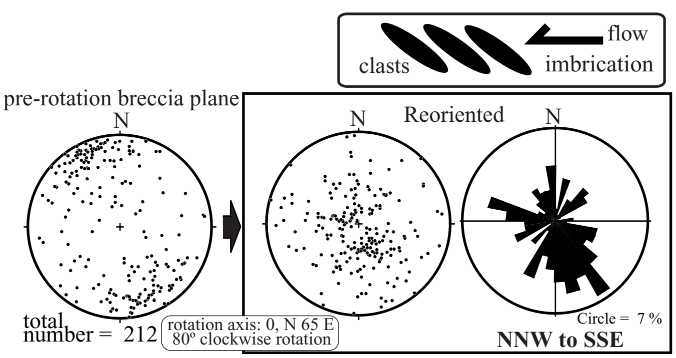

Figure 10. Paleocurrent direction for Lower Breccia Member. Plot shows dip and strike of disk-shaped clast, which preserved similar direction. Note data reoriented 70° clockwise by N65E horizontal axis.

Analytical methods

Isolation of grains. We fragmented ~100 samples of calcarenite, weighing ~50 g each, to a grain size of 1 cm to few millimeters. The samples were then treated with dilute hydrochloric acid for ~30 min and after complete dissolution of the carbonate material, the residue was magnetically separated into magnetic, weak magnetic, and nonmagnetic grains. Thin sections of the three kinds of residues (~1–3 g) were prepared, and these thin sections were used for counting and measuring grains under optical and electron microscopes. The composition of the grains was determined by EDS or EPMA.

The nonmagnetic residue of shocked quartz was treated with silica-saturated hydrofluorosilicic acid for three days, so that other minerals were completely dissolved. After making a thin section of the new residue, we produced a grain map of the thin section in a slide scanner. These scanner images make it easy to identify the normal and deformed quartz. Shocked quartz was identified by the presence of more than two sets of planar deformation features (PDFs: Fig. 11, A, B, and C), which have distinct angles from the c-axis in the quartz (e.g., Stöffler and Langenhorst, 1994; French, 1998). When looking for deformed quartz on a map, we try to measure the PDFs, which are characterized by at least two sets of straight planar features. We exclude the spaced and planar fracture (PF) structures formed at this stage. Measuring the orientation of the PDFs of quartz in the thin section was performed on a universal stage (e.g., Montanari and Koeberl, 2000), and then plotted in frequency distribution histograms.

We processed the magnetically separated residue to obtain spherules. Spherules were searched for under a stereomicroscope, then the spherule surfaces were observed by electron microscopy. At this stage, we picked up only smooth spherules. After we examined the spherule surfaces, each grain was glued to a slide glass and we made half-cut polished sections for observation by EDS and EPMA. Microfossils such as radiolaria, ostracoda, and foraminifera were distinguished at this stage. The radiolaria, which are totally replaced with goethite, have round tests with well-regulated small openings and are very common in this formation. The ostracoda and foraminifera were preserved only as lattice shapes replaced by oblong clay minerals.

Shocked quartz

Shocked quartz is found throughout the Cacarajicara Formation (Fig. 4). PDF orientation has been used as a shock barometer to measure the intensity and distribution of shock pressures (Grieve and Robertson, 1976; Dressler and Sharpton, 1997) Most of the PDFs in the shocked quartz from this formation are concentrated at the ω (23°), π (32°), ζ (48°), and γ (52°) positions from the c-axis of quartz crystals (Fig. 12). The presence of the π plane with a number of different orientation

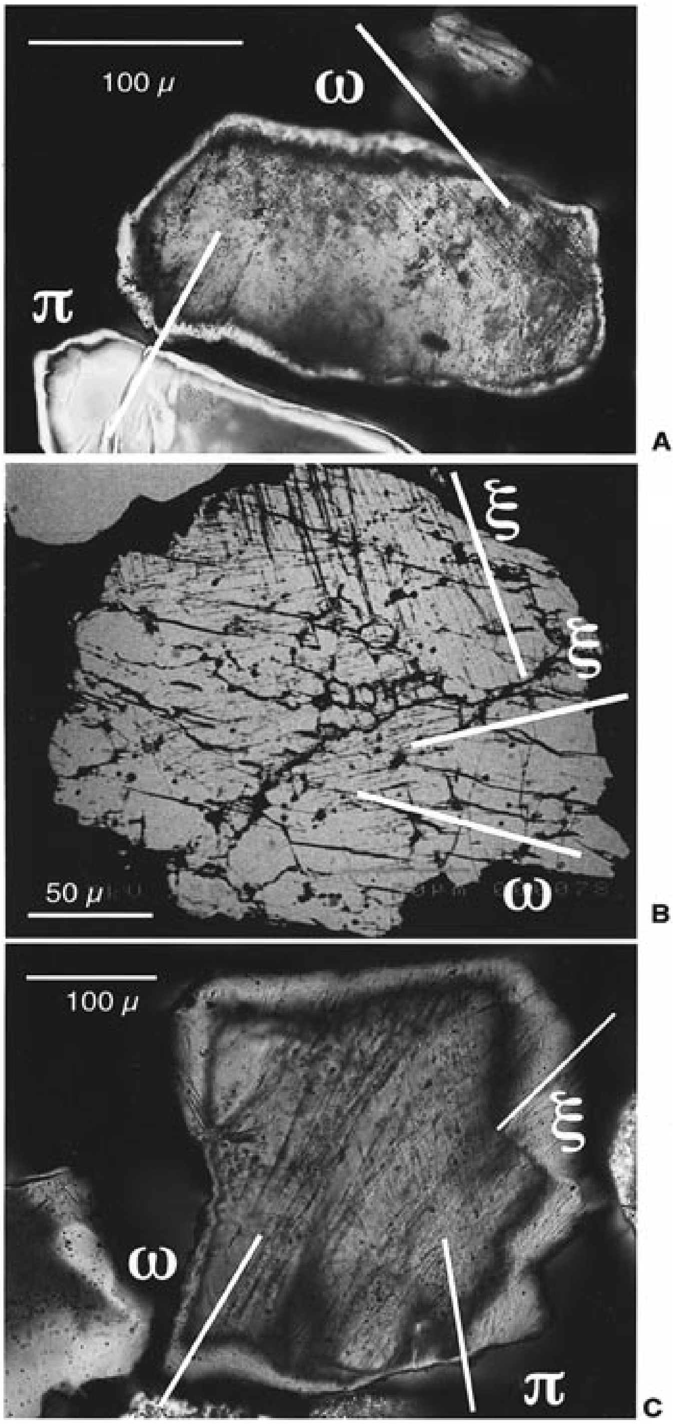

Figure 11. A: Planar deformation features (PDFs) in shocked quartz (crossed nicols) from Middle Calcarenite Member (sample 98-18). PDF shows ω and π planes. B: Backscattered electron (BSE) image of shocked quartz in Middle Calcarenite Member (sample 99-4). PDF shows ω and ζ planes, as measured on universal stage by microscope. C: PDFs in shocked quartz (crossed nicols) in Lower Breccia Member (sample Mx-1). PDF shows π, ζ, and ω planes.

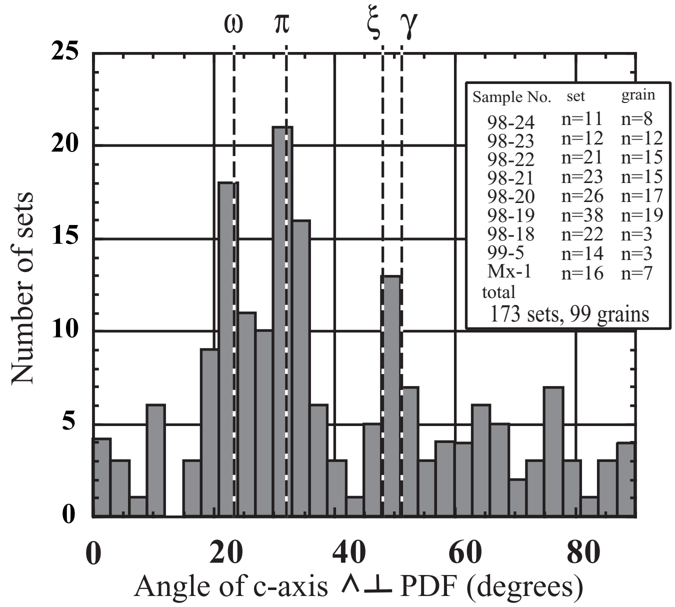

Figure 12. Shocked-quartz planar deformation feature (PDF) orientation diagram.

planes suggests that the shocked quartz in the Cacarajicara Formation was affected by more than 16 GPa of pressure.

The abundance of shocked quartz with PDFs in the Cacarajicara Formation varies from <20% to 7% of total quartz grains in the acid-dissolved residue (Fig. 4). The matrix in the basal part of the Lower Breccia Member and the fine sand-size calcarenite in the upper Middle Calcarenite Member preserve shocked quartz in abundances as high as 15%–20% of the total number of quartz grains.

Spherules

The identity of impact-related spherules in the Cacarajicara Formation is still not known with certainty. However, the matrix in the basal part of the Lower Breccia Member contains three types of spherules. The first type of spherule is gray, 200–300 µm in diameter, and has a very smooth surface and partly elongated shape (Fig. 13A). Based on backscattered electron images and EDS analysis, this type of spherule is composed of homogeneous clay minerals, mainly smectite. It may be an altered glass spherule. The second type of spherule consists of isolated silica spheroids preserved in the clay matrix within the basal Lower Breccia Member (Fig. 8B). These spherules are well rounded and are formed of a quartz crystal with radical extinction (Fig. 13B). The third spherule type consists of goethite, which is distinguished by some larger (500–1000 µm in diameter) and other smaller (200–300 µm in diameter) spherules (Fig. 8C). The larger spherules are similar in size to those in the Beloc samples (Izett, 1991; Bohor and Glass, 1995). The surface of the goethite spherules is a smooth and irregular plane.

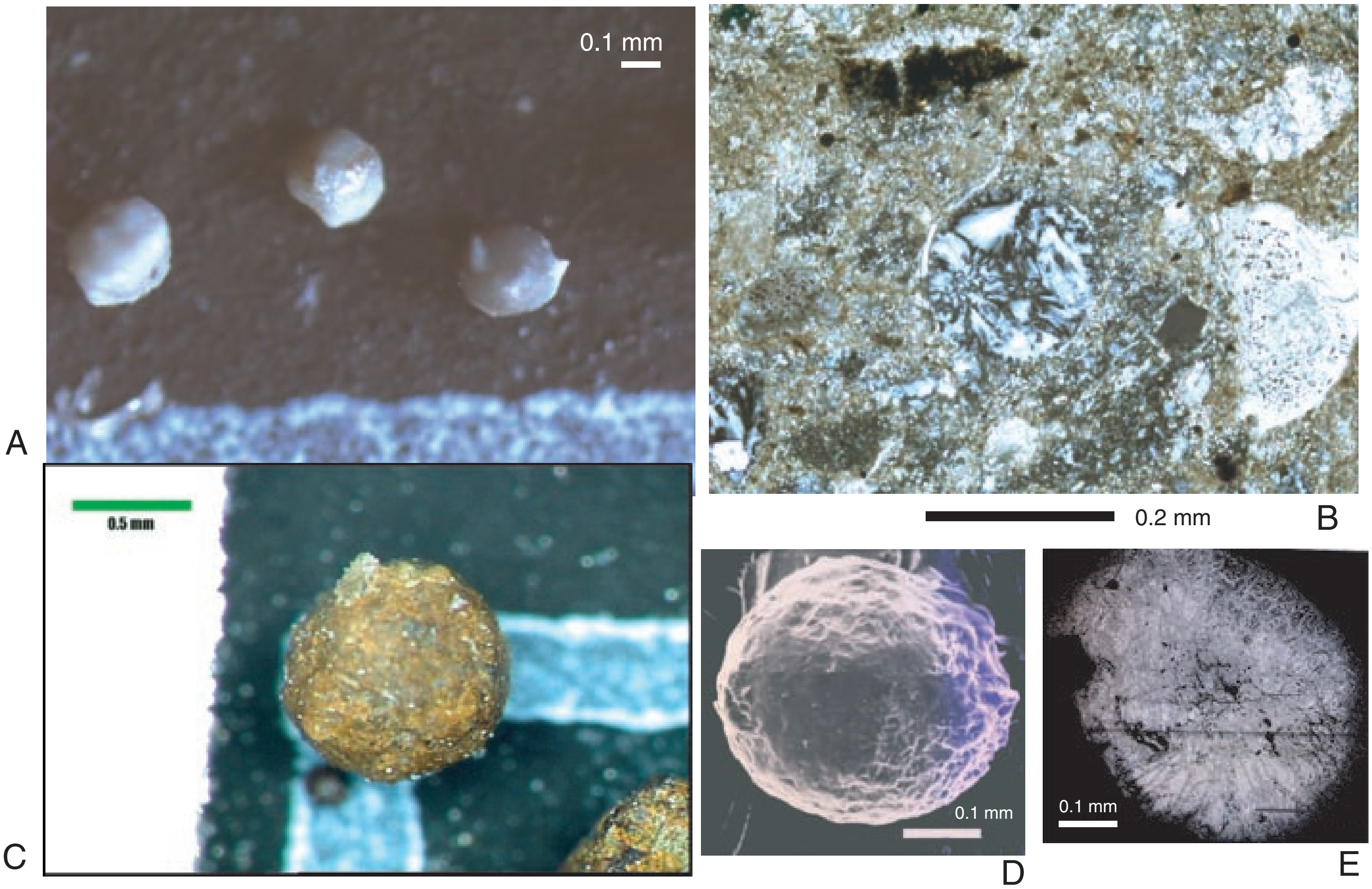

Figure 13. A: Gray spherules in matrix of Lower Breccia Member (0.3 mm in diameter, sample Mx-1). Note smectite in each grain. B: Silica-rich spherules in matrix of Lower Breccia Member (0.3 mm diameter). C: Large goethite spherules (sample Mx-1). D: Scanning electron microscope (SEM) image of gray spherule surface (sample Mx-1). E: SEM image of section of goethite spherules (sample Mx-1). Note dendritic texture preserved and overprinted by goethite.

The insides of large goethite spherules are very homogeneous and partly preserve a dendritic texture (Fig. 13E) that resembles the texture seen in the second type of spherule that has been entirely replaced by goethite (Bohor and Glass, 1995).

Carbonate pisoliths

The carbonate pisoliths are well preserved in matrix of the middle-fine calcarenite of the Middle Calcarenite Member (Fig. 9D). The matrix is formed of simple 200–300-µm-diameter calcite crystals within a fibrous radial structure. These pisoliths have 1-µm-thick calcite wall that forms perfect spheres. This is a simpler crystal than the laminated ooids or microfossils, and it is not preserved in the other carbonate clasts or carbonate grains. Similar pisoliths are also contained in the matrix within the middle member of the Peñalver Formation, which was not metamorphosed. Calcite pisoliths in the spherule layer on Albion Island are 7–10 mm in diameter, larger than in the Cacarajicara Formation. However, a radial structure with 1–2-mm-thick shells is also present (Pope et al., 1999). The carbonate pisoliths in the Middle Calcarenite member might have been formed as accretional carbonate tuff from impact-induced calcite vapor.

DISCUSSION

Here we review the origin, transportation, and depositional mechanisms of the Cacarajicara Formation. The upward-fining sequence in this formation was likely formed by one gravity flow event. The sedimentary characteristics, however, are very different from those seen in normal turbidite and debris-flow deposits. We have focused on the flow characteristics of each member of this thick formation in order to infer flow transportation mechanisms, and relate these to the Chicxulub impact.

Transportation mechanisms

Lower Breccia Member. The clasts in the Lower Breccia Member have shallow-water, deep-water, and orogenic belt origins. Many limestone and chert breccias resemble those in underly-

ing Cretaceous formations. The thick mixed-clast member may represent a collapse of the continental margin of the Yucatan platform. We proposed that these thick clasts are transported by laminar flow for the following reasons.

The cobble- to pebble-size clasts in the Lower Breccia Member are mostly in direct contact with each other and are similar to those in other grain-flow deposits (Bagnold, 1954). Such clasts were affected by the high dispersive pressure of grain collisions. The grain-boundary conditions around the clay matrix, however, preserved hydrofractured clasts, cracked chert clasts, and matrix intrusion structures within limestone clasts. The pebble-size carbonate present in the matrix alongside large boulders, which can be regarded as flow shadows, is preserved as a highly fractured fabric. There is no evidence that the other cobble- to boulder-size clasts were similarly influenced by this flow shadow. These features imply a high pore-pressure condition in this matrix, and the large clasts were fractured by the hydrostatic conditions.

The flow behavior of grain-supported sediments is changed by flow speed (Pierson and Costa, 1987). Grain-supporting mechanisms, such as the turbulence, dispersive stress, and fluidization, increase with flow velocity. In this way, with increasing pore pressure of the flow matrix, the grains floated and were transported long distances (e.g., Shanmugam, 1996). The Lower Breccia Member contains the following characteristics: (1) the reverse-graded and imbricated fabrics of the boulder clasts show the shear distribution of flow; (2) direct contact between each clast implies a high dispersive pressure condition; and (3) many matrix intrusions and a mosaic or jigsaw puzzle texture alongside limestone clasts also indicate high pore pressures. These features suggest that the Lower Breccia Member formed under laminar flow conditions in a very high speed dilatant situation (Lowe, 1976; Todd, 1989; Shanmugam, 1996).

Middle Calcarenite Member. The homogeneous and well-sorted calcarenite with deep- and shallow-origin rocks implies that the Middle Calcarenite Member formed under extremely mixed, strongly turbulent conditions. Sustained steady or quasi-steady current and upward migration of a depositional flow were required to form such a thick, massive calcarenite with a homogeneous fabric and large-scale grading. This process is referred to as high-density turbidity suspension (Kneller and Branney, 1995). The diffused flow laminations in the massive and well-sorted facies also suggest that the grains belonged to a strong suspension (deposit) environment, rather than a flow (shear) environment. The many fluid-escape structures also suggest that the deposit was formed by fast loading of high-density sediments under overpressured conditions. This evidence implies that the member formed from a high-density turbidity suspension.

Upper Lime Mudstone Member. The fine-grained Upper Lime Mudstone Member was probably deposited from a dilute sedimentary suspension. The gradually changing grain size and composition from those seen in the Middle Calcarenite Member suggest that the Upper Lime Mudstone Member was formed by a continuous, more dilute suspension.

Takayama et al. (2000), however, proposed “homogenite,” which is formed by a tsunami, for the middle member of the Peñalver Formation. The Middle Calcarenite Member preserves sedimentary features that are similar to those in the Peñalver Formation. A tsunami produces mixing and turbidity in ocean sediments and may occur with or slightly after gravity sliding and ejecta flow. The very thick high-density turbidity suspension might have been produced tsunami-induced remixing. However, it is unknown whether the Cacarajicara Formation was influenced by a tsunami wave.

Relationship to the Chicxulub impact. The presence of shocked quartz and microspherules indicates that the Cacarajicara Formation resulted from an impact. The paleocurrent distribution inferred from the boulder imbrication in the Lower Breccia Member shows a north-northwest to south-southeast direction in modern terms. The Rosario belt belongs to an orogenic terrane, and the basic structure is top-to-the-north vergence with east-west-striking folds and thrusts (Gordon et al., 1997). It is difficult to rotate bedding 180° inside such an orogenic belt, so we propose that this paleocurrent flow came from the depositional area. When the Guaniguanico terrane of western Cuba is restored to its original orientation at the K-T interval, the Cacarajicara Formation was situated on the southeastern margin of the Yucatan Peninsula (Pindell et al., 1988; Ross and Scotese, 1988). In this position, the south-southeast direction of paleocurrents is consistent with the former location of the Yucatan continental margin.

Sedimentation model

Clastic rocks of the Cacarajicara Formation mainly originated from the collapse of the Yucatan platform (Fig. 14). The deep-water limestone and black chert, which are main components of this formation, represent continental slope deposition, whereas shallow-water limestone such as rudist and oolite limestones and dolomite represent platform margin deposition. The volcanic and metamorphic rocks are also present in the San Cayetano Formation and the Roble member of the Polier Formation, which were also located on the continental margin or slope along the Yucatan platform.

The inferred sedimentation of the Cacarajicara Formation, which records laminar flow, high-turbidite suspension, and diluted suspension, resembles the hyperconcentrated flow that has been associated with high-energy and high-speed flows (Pierson and Costa, 1987). These sedimentary characteristics of the Cacarajicara Formation are similar to those of deposits produced by a subaqueous eruption (White, 2000). Subaqueous-eruption flow deposits are also composed of three layers; in ascending order, these are a grain-supported high concentration of rocks that is identified with high-concentration laminar flow, a massive to stratified, graded, volcaniclastic sandstone layer that formed from a high-concentration turbidite flow, and a fine-

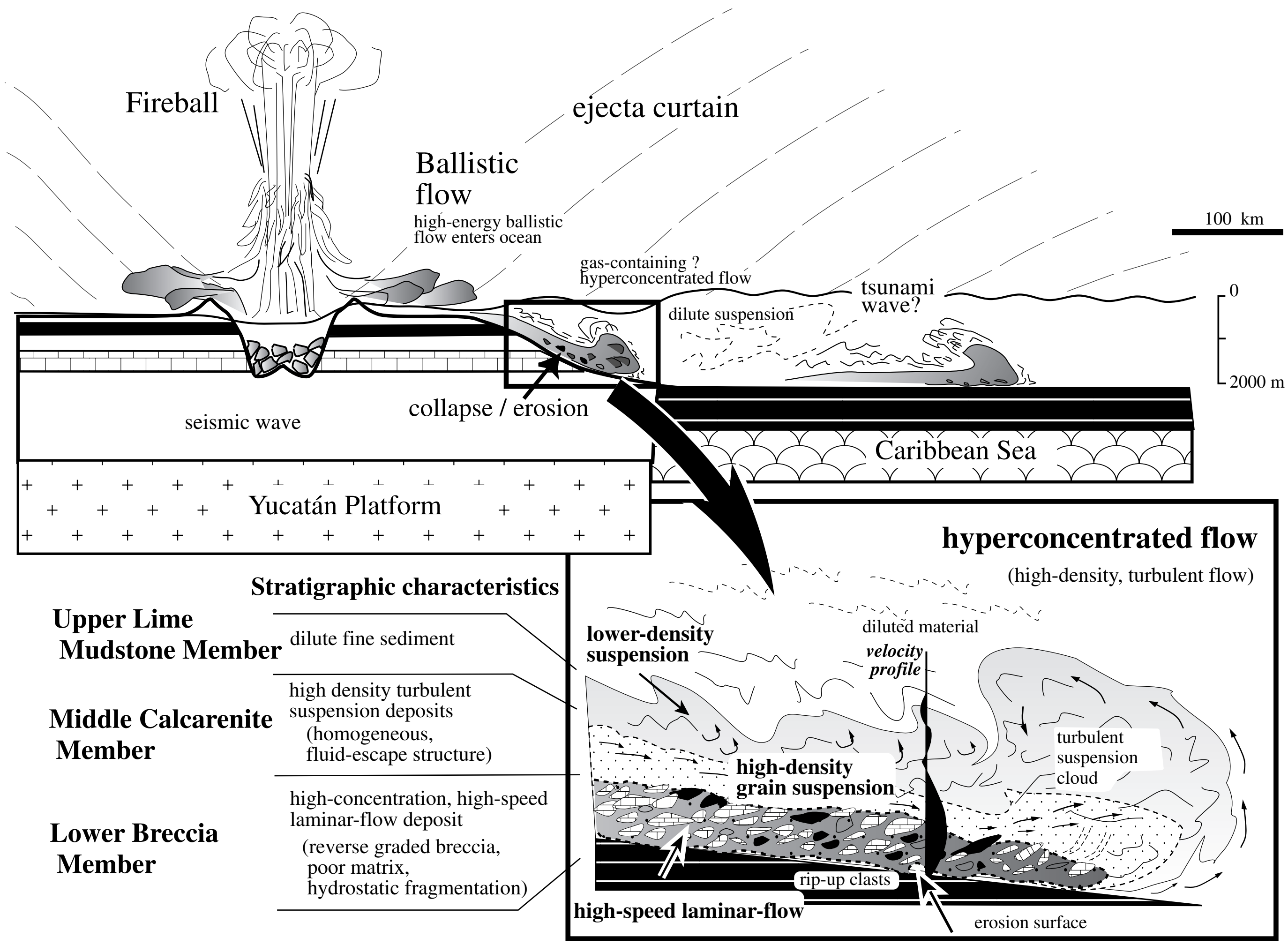

Figure 14. Schematic sedimentation model of Cacarajicara Formation. Note that impact-related shock waves and ballistic flows created gigantic hyperconcentrated flow. Flow consists of three different flow units that formed three sedimentary facies sequences: high-speed laminar-flow clasts, high-density turbulent-suspension deposits, and low-density, diluted, fine material. Middle and upper sequences might have been affected by tsunami wave mixing.

grained tuffaceous layer that formed a dilute low-density suspension (Mueller and White, 1993). The subaqueous eruption flows are products of high-energy flow and suspension deposition in the deep sea. The stratified middle sequence of the subaqueous eruption flow, however, is different from that of the Cacarajicara Formation, which preserves a homogeneous calcarenite sequence. The massive, homogeneous calcarenite sequence of the Cacarajicara Formation has a more mixed and suspended character.

One possibility is that an extraordinary gravity flow was triggered by an impact-related earthquake, keeping in mind that the estimated collapse locality of the Yucatan platform margin is more than 500 km from the impact site. The arrival of the seismic wave (at 5–7 km/s) would occur ~2 min after the arrival of impact ballistic flows (the initial blast is 30 km/s and main body of the vapor cloud is 10 km/s or less) (Melosh, 1989). This suggests that the seismic shock wave and ballistic flows arrived almost simultaneously.

As described here, the Cacarajicara Formation is a high-energy flow deposit that was formed by platform collapse resulting from an impact-related seismic wave and ballistic flow. This flow transported the shallow- (continental shelf) and deep-water (continental slop) sediments of the Yucatan platform margin to the deep Yucatan ocean basin. As evidenced by the thick homogeneous calcarenite, such a gigantic flow would have been very turbulent. An immense tsunami resulting from the impact might have mingled with this turbulence to form the very thick homogeneous calcarenite sequence.

CONCLUSIONS

The Cacarajicara Formation is a >700-m-thick calcareous sedimentary sequence that fines upward. This formation con-

tains Maastrichtian fossils (foraminifera), and impact-related shocked quartz and spherules. Three members are identified in this formation. The Lower Breccia Member consists of a matrix-poor breccia sequence formed by high-energy lamina-flow. The Middle Calcarenite Member is characterized by well-sorted homogeneous calcarenite that was deposited from a high-concentration sediment suspension. The Upper Lime Mudstone Member is composed of massive, fine calcarenite-lime mudstone, which was deposited from a dilute suspension. The gradual transition between the three members of the Cacarajicara Formation can be explained by high-energy hyperconcentrated flow. Alternatively, the upper half of the formation can be interpreted as a deep-sea tsunami deposit (homogenite) similar to that in the upper half of the Peñalver Formation. The presence of shallow- and deep-water facies clasts, shocked quartz, spherules, and a south-southeast-trending paleocurrent suggest that this flow was formed by Chicxulub impact-related, seismically induced gravity flow combined with impact ballistic flow. Therefore, the Cacarajicara Formation is one of thickest sequences resulting from the gigantic Chicxulub impact-induced flow.

ACKNOWLEDGMENTS

We thank Agencia Medio Ambiente, Cuba, for their support of field survey in Cuba. This research was made possible by an agreement between the Department of Earth and Planetary Sciences, the University of Tokyo, and the Museo Nacional de Historia Natural (Agencia del Medio Ambiente) de Cuba and el Instituto de Geologia del Ministerio del Industria Basica. Y. Saito, K. Yokoyama, and colleagues of the National Science Museum of Japan are acknowledged for their suggestions and for using the energy-dispersive spectrometer and electron probe microanalyzer analysis. A. Taira provided useful discussions and provided helpful suggestions. We acknowledge the important support provided to field research in Cuba by Mitsui & Co., Ltd., as well as their manager in Havana, A. Nakata. We thank Christian Koeberl, Michael Rampino, and an unknown reader for constructive and insightful reviews. The survey was supported by research funds donated to University of Tokyo by NEC Corp., I. Ohkawa, M. Iizuka, and K. Ihara. This study was partly supported by a grant-in-aid (11691116) for scientific research from the Japan Society for the Promotion of Science.

REFERENCES CITED

Alvarez, W., Smit, J., Lowrie, W., Asaro, F., Margolis, S.V., Claeys, P., Kastner, M., and Hildebrand, A.R., 1992, Proximal impact deposits at the Cretaceous-Tertiary boundary in the Gulf of Mexico: A restudy of DSDP Leg 77 Site 536 and 540: Geology, v. 20, p. 697–700.

Bagnold, R.A., 1954, Experiments on a gravity-free dispersion of large solid spheres in a Newtonian Fluid under shear: Proceedings of the Royal Society, London, ser. A, v. 225, p. 49–63.

Bohor, B.F., and Seitz, R., 1990, Cuban K/T catastrophe: Nature, v. 344, p. 593.

Bohor, B.F., and Glass, B.P., 1995, Origin and diagenesis of K/T impact spherules: From Haiti to Wyoming and beyond: Meteoritics, v. 30, p. 182–198.

Bohor, B.F., 1996, Sediment gravity flow hypothesis for siliciclastic units at the K/T boundary, northeastern Mexico, *in* Ryder G., Fastovsky D., and Gartner, S., eds., The Cretaceous-Tertiary event and other catastrophes in Earth history: Geological Society of America Special Paper 307, p. 183–195.

Bourgeois, J., Hansen, T.A., Wiberg, L., and Kauffman, E.G., 1988, A tsunami deposit at the Cretaceous-Tertiary boundary in Texas: Science, v. 241, p. 567–570.

Bralower T.J., and Iturralde-Vinent M., 1997, Micropaleontological dating of the collision between the North American Plate and the Greater Antilles Arc in Western Cuba: Palaios, v. 12, p. 133–150.

Bralower, T.J., Paull, C.K., and Leckie, R.M., 1998, The Cretaceous-Tertiary boundary cocktail: Chicxulub impact triggers margin collapse and extensive sediment gravity flows: Geology, v. 26, p. 331–334.

Bronnimann P., and Rigassi, D., 1963, Contribution to the geology and paleontology of the city of La Habana, Cuba, and its surroundings: Eclogae Geologicae Helvetiae, v. 56, p. 193–480.

Dressler, B.O., and Sharpton, V.L., 1997, Breccia formation at a complex impact crater: Slate Island, Lake Superior, Ontario Canada: Tectonophysics, v. 275, p. 285–311.

French, B.M., 1998. Traces of catastrophe: A handbook of shock-metamorphic effects in terrestrial meteorite impact structures: Houston, Texas, Lunar and Planetary Institute, LPI Contribution No. 954, 120 p.

Gordon, M.B., Mann, P., Caceres, D., and Flores, R., 1997, Cenozoic tectonic history of the North America-Caribbean plate boundary zone in western Cuba: Journal of Geophysical Research, v. 102, p. 10055–10082.

Grajales-Nishimura, J.M., Cedillo-Pardo, E., Rosales-Dominguez, C., Moran-Zenteno, D.J., Alvarez W., Claeys P., Ruiz-Morales J., Garcia-Hernandez J., Padilla-Avila P., and Sanchez-Rios, A., 2000, Chicxulub impact: The origin of reservoir and seal facies in the southeastern Mexico oil fields: Geology, v. 28, p. 307–310.

Grieve, R.A., and Robertson, P.B., 1976, Variations in shock deformation at the Slate Islands impact structure, Lake Superior, Canada: Contribution to Mineralogy and Petrology, v. 58, p. 37–49.

Hildebrand, A.R., Penfield, G.T., Kring. D.A., Pilkington, M., Camargo, Z.A., Jacobsen S.B., and Boynton, W.V., 1991, Chicxulub crater: A possible Cretaceous/Tertiary boundary impact crater on the Yucatan Peninsula, Mexico: Geology, v. 19, p. 867–871.

Iturralde-Vinent, M.A., 1992, A short note on the Cuban late Maastrichtian megaturbidite (and impact-derived deposit?): Earth and Planetary Science Letters, v. 109, p. 225–228.

Iturralde-Vinent, M.A., 1994a, Cuban geology: A new plate-tectonic synthesis: Journal of Petroleum Geology, v. 17, p. 39–70.

Iturralde-Vinent, M.A., 1994b, Interrelationship of the terranes in western and central Cuba: Comment: Tectonophysics, v. 234, p. 345–348.

Iturralde-Vinent, M.A., 1996, Introduction to Cuban geology and tectonics, *in* Iturralde-Vinent, M.A., ed., Ofiolitas y arcos volcanicos de Cuba (Cuban ophiolites and volcanic arcs): Miami, Florida, International Geological Correlation Programme 364, p. 3–23.

Izett, G.A., 1991, Tectites in Cretaceous-Tertiary Boundary rocks on Haiti and their bearing on the Alvarez impact extinction hypothesis: Journal of Geophysical Research, v. 96, p. 20879–20905.

Kerr, A.C., Iturralde-Vinent, M.A., Saunders, A.D., Babbs, T.L., and Tarney, J., 1999, A new plate tectonic model of the Caribbean: Implications from a geochemical reconnaissance of Cuban mesozoic volcanic rocks: Geological Society of America Bulletin, v. 111, p. 1581–1599.

Kneller, B.C., and Branney, M.J., 1995, Sustained high-density turbidity currents and the deposition of thick massive sands: Sedimentology, v. 42, p. 607–616.

Lowe, D.R., 1976, Grain flow and grain flow deposits: Journal of Sedimentary Petrology, v. 46, p. 188–199.

Melosh, H.J., 1989, Impact cratering: A geologic process: Oxford, UK, Oxford University Press, 245 p.

Montanari, A., and Koeberl, C., 2000. Impact stratigraphy: The Italian record *in* Bhattacharji, S., Friedman, G.M., Neugebauer H.J., and Seilacher, A., eds., Lecture notes in earth sciences, Volume 93: Berlin, Springer-Verlag, 364 p.

Mueller, W., and White, J.D.L., 1993, Felsic fire-fountaining beneath Archean seas: Pyroclastic deposits of the 2730 Ma Hunter Mine Group, Quebec, Canada: Journal of Volcanology Geothermal Research, v. 54, p. 117–134.

Oberbeck, V.R., 1975, The role of ballistic erosion and sedimentation in lunar stratigraphy: Reviews of Geophysics Space Physics, v. 13, p. 337–362.

Ocampo, A.C., Pope, K.O., and Fischer, A.G., 1996, Ejecta blanket deposits of the Chicxulub crater from Albion Island, Belize, *in* Ryder G., Fastovsky D., and Gartner, S., eds., The Cretaceous-Tertiary event and other catastrophes in Earth history: Geological Society of America Special Paper 307, p. 75–88.

Palmer, R.H., 1945, Outline of the geology of Cuba: Journal of Geology, v. 53, p. 1–34.

Pierson, T.C., and Costa, J.E., 1987 A rheologic classification of subaerial sediment-water flows, *in* Costa, J.E., and Wieczorek, G.F., eds., Debris flows/avalanches: Process, recognition, and mitigation: Reviews in Engineering Geology, v. 7, p. 1–12.

Pindell, J.L., and Barrett, S.F., 1990, Geologic evolution of the Caribbean region: A plate-tectonic perspective, *in* Dengo, G., and Case, J.E., eds., The Caribbean Region: Boulder, Colorado, Geological Society of America, Geology of North America, v. H, p. 405–432.

Pindell, J.L., Cande, S.C., and Pitman, W.C., III, Rowley, D.B., Dewey, J.F., Labercque, J., and Haxby W., 1988, A plate-kinematic framework for models of Caribbean evolution: Tectonophysics, v. 155, p. 121–138.

Piotrowska, K., 1993. Interrelationship of the terranes in western and central Cuba: Tectonophysics, v. 220, p. 273–282.

Pope, K.O., Ocampo, A.C., Fischer, A.G., Alvarez, W., Fouke, B.W., Webster, C.L., Vega, F.J., Smit, J., Fritsche, A.E., and Claeys, P., 1999, Chicxulub impact ejecta from Albion Island, Belize: Earth and Planetary Science Letters, v. 170, p. 351–364.

Pszczolkowski, A., 1978, Geosynclinal sequences of the Cordillera de Guaniguanico in western Cuba: Their lithostratigraphy, facies development and paleogeography: Acta Geological Polish, v. 28, p. 1–96.

Pszczolkowski, A., 1986, Megacapsa del maestrichitiano de Cuba occidental y central: Bulletin of Polish Academic of Earth Science, v. 34, p. 81–87.

Pszczolkowski, A., 1994, Interrelationship of the terranes in western and central Cuba: Comment: Tectonophysics, v. 234, p. 339–344.

Pushcharovsky, Y., 1989, Geology of Cuba, Explanatory note to the 1:250 000 geological map of Cuba: Moscow, Geological Institute of the USSR Academy of Sciences, Nauka, 55 p.

Rosencrants, E., 1990, Structure and tectonics of the Yucatan basin, Caribbean Sea, as determined from seismic reflection studies: Tectonics, v. 9, p. 1037–1059.

Ross, M.I., and Scotese, C.R., 1988, A hierarchical tectonic model of the Gulf of Mexico and Caribbean region: Tectonophysics, v. 155, p. 139–168.

Shanmugam, G., 1996, High-density turbidity currents: Are they sandy debris flows?: Journal of Sedimentary Research, v. 66, p. 2–10.

Sharpton, V.L., Dalrymple, G.B., Marin, L.E., Ryder, G., Schuraytz, B.C., and Urrutia-Fucugauchi, J., 1992, New links between the Chicxulub impact structure and the Cretaceous/Tertiary boundary: Nature, v. 359, p. 819–821.

Sharpton, V.L., Martin, L.E., Carney, J.L., Ryder, G.S., Scjiraytz, C.S, Sikora, P., and Spudis, P.D., 1996, A model of the Chicxulub impact basin based on evaluation of geophysical data, well logs and drill core samples, *in* Ryder, G., Fastovsky, D., and Gartner, S., eds., The Cretaceous-Tertiary event and other catastrophes in Earth history: Geological Society of America Special Paper 307, p. 55–74.

Smit, J., 1999, The global stratigraphy of the Cretaceous-Tertiary boundary impact ejecta: Annual Reviews of Earth and Planetary Science, v. 27, p. 75–113.

Smit, J., Reop, R.B., Alvarez, W., Montanari, A., Claeys, P., Grajales-Nishimura, J.M., and Bermudez, J., 1996, Coarse-grained, clastic sandstone complex at the K/T boundary around the Gulf of Mexico: Deposition by tsunami waves induced by the Chicxulub impact?, *in* Ryder, G., Fastovsky, D., and Gartner, S., eds., The Cretaceous-Tertiary event and other catastrophes in Earth history: Geological Society of America Special Paper 307, p. 151–182.

Stöffler, D., and Langenhorst, F., 1994, Shock metamorphism of quartz in nature and experiment. 1. Basic observation and theory: Meteoritics, v. 29, p. 155–181.

Takayama, H., Tada, R., Matsui, T., Iturralde-Vinent, M.A., Oji, T., Tajika, E., Kiyokawa, S., Garcia, D., Okada, H., Hasegawa, T., and Toyoda, K., 2000, Origin of the Peñalver Formation in northwestern Cuba and its relation to K/T boundary impact event: Sedimentary Geology, v. 135, p. 295–320.

Todd, S.P., 1989, Stream-driven high-density gravelly traction carpets: Possible deposits in the Trabeg Conglomerate Formation, SW Ireland and theoretical considerations of their origin: Sedimentology, v. 36, p. 513–530.

Yokoyama, K., Matsubara, S., Saito, Y., Tiba, T., Kato, A., 1993. Analyses of natural minerals by energy-dispersive spectrometer: Bulletin of National Science Museum of Tokyo, ser. C. v. 10, p. 115–126.

White, J.D.L., 2000, Subaqueous eruption-fed density currents and their deposits: Precambrian Research, v. 101, p. 87–109.

Manuscript Accepted by the Society March 22, 2001